

Internal Energy of Molecules Ejected Due to Energetic C₆₀ Bombardment

Barbara J. Garrison,^{*,†} Zbigniew Postawa,[‡] Kathleen E. Ryan,[†] John C. Vickerman,[§] Roger P. Webb,^{||} and Nicholas Winograd[†]

Department of Chemistry, 104 Chemistry Building, Pennsylvania State University, University Park, Pennsylvania 16802, Smoluchowski Institute of Physics, Jagiellonian University, ul. Reymonta 4, 30-059 Kraków, Poland, Manchester Interdisciplinary Biocentre, The School of Chemical Engineering and Analytical Science, The University of Manchester, M1 7ND, United Kingdom, and Department of Electronic and Electrical Engineering, University of Surrey, Guildford, GU2 5XH, United Kingdom

The early stages of C₆₀ bombardment of octane and octatetraene crystals are modeled using molecular dynamics simulations with incident energies of 5–20 keV. Using the AIREBO potential, which allows for chemical reactions in hydrocarbon molecules, we are able to investigate how the projectile energy is partitioned into changes in potential and kinetic energy as well as how much energy flows into reacted molecules and internal energy. Several animations have been included to illustrate the bombardment process. The results show that the material near the edge of the crater can be ejected with low internal energies and that ejected molecules maintain their internal energies in the plume, in contrast to a collisional cooling mechanism previously proposed. In addition, a single C₆₀ bombardment was able to create many free and reacted H atoms which may aid in the ionization of molecules upon subsequent bombardment events.

The use of energetic cluster beams such as C₆₀ in secondary ion mass spectrometry (SIMS) has introduced new physical processes into the mechanism by which intact molecules are emitted from surfaces.^{1,2} Experimentally, these clusters remove massive amounts of material^{3–8} and, importantly, can increase the ion fraction of molecular species over atomic bombardment.⁹ There is experimental and computational evidence that the mechanisms of material removal due to energetic cluster bom-

bardment are distinct from energetic atomic bombardment.^{10–14} In particular, the motion of the atoms in a C₆₀ projectile is correlated so that the C₆₀ molecule at first acts like a single large particle when hitting the sample and creates a crater.¹⁵ The large size of the C₆₀ projectile and the disorder created around the edge of the crater tend to inhibit individual carbon atoms originating from the projectile from penetrating deep into the sample.¹⁶ Therefore, the energy from the projectile can only be deposited to the sample in the near-surface region where it will contribute to an enhanced yield and also restrict the damaged molecules to the near-surface region.

Given that molecular solids are a pinnacle application of cluster SIMS especially by C₆₀ bombardment, a microscopic view of the process is desirable. Previous molecular dynamics (MD) simulations of C₆₀ bombardment have focused primarily on atomic systems^{16–19} or rigid molecular systems^{11,20,21} where the bond lengths are not allowed to stretch or break. These restrictions lend themselves to the use of simpler potentials and larger time steps in simulations, therefore decreasing the computation time required to complete a full simulation. A few exceptions lie in simulations of cluster bombardment of water using a dissociative potential²² and coarse-grained organics such as benzene^{23–27} and various polymers.^{28,29} In the first case, water was described by a potential that allowed each molecule to break into H⁺, OH[–], or O^{2–} ions but not into any neutral species. In addition, the

* To whom correspondence should be addressed. E-mail: bjg@psu.edu.

[†] Pennsylvania State University.

[‡] Jagiellonian University.

[§] The University of Manchester.

^{||} University of Surrey.

- (1) Castner, D. G. *Nature* **2003**, *422*, 129.
- (2) Winograd, N. *Anal. Chem.* **2005**, *77*, 142A.
- (3) Szakal, C.; Kozole, J.; Russo, M. F., Jr.; Garrison, B. J.; Winograd, N. *Phys. Rev. Lett.* **2006**, *96*, 216104.
- (4) Shard, A. G.; Green, F. M.; Brewer, P. J.; Seah, M. P.; Gilmore, I. S. *J. Phys. Chem. B* **2008**, *112*, 2596–2605.
- (5) Cheng, J.; Wucher, A.; Winograd, N. *J. Phys. Chem. B* **2006**, *110*, 8329.
- (6) Sostarecz, A. G.; Sun, S.; Szakal, C.; Wucher, A.; Winograd, N. *Appl. Surf. Sci.* **2004**, *231–2*, 179.
- (7) Wucher, A.; Sun, S.; Szakal, C.; Winograd, N. *Anal. Chem.* **2004**, *76*, 7234.
- (8) Möllers, R.; Tuccitto, N.; Torrisi, V.; Niehuis, E.; Licciardello, A. *Appl. Surf. Sci.* **2006**, *252*, 6509–6512.
- (9) Weibel, D.; Wong, S.; Lockyer, N.; Blenkinsopp, P.; Hill, R.; Vickerman, J. C. *Anal. Chem.* **2003**, *75*, 1754.

- (10) Sun, S.; Szakal, C.; Wucher, A.; Winograd, N. *J. Am. Soc. Mass Spectrom.* **2005**, *16*, 1677.
- (11) Wojciechowski, I. A.; Garrison, B. J. *J. Phys. Chem. A* **2006**, *110*, 1389.
- (12) Garrison, B. J.; Postawa, Z. *Mass Spectrom. Rev.* **2008**, *27*, 289.
- (13) Webb, R. P.; Kerford, M.; Kappes, M.; Brauchle, G. *Nucl. Instrum. Methods Phys. Res., Sect. B* **1997**, *318–321*.
- (14) Kerford, M.; Webb, R. P. *Nucl. Instrum. Methods Phys. Res., Sect. B* **2001**, *180*, 44.
- (15) Garrison, B. J.; Ryan, K. E.; Russo, M. F.; Smiley, E. J.; Postawa, Z. *J. Phys. Chem. C* **2007**, *111*, 10135.
- (16) Postawa, Z.; Czerwinski, B.; Szewczyk, M.; Smiley, E. J.; Winograd, N.; Garrison, B. J. *J. Phys. Chem. B* **2004**, *108*, 7831.
- (17) Postawa, Z.; Czerwinski, B.; Szewczyk, M.; Smiley, E. J.; Winograd, N.; Garrison, B. J. *Anal. Chem.* **2003**, *75*, 4402.
- (18) Krantzman, K. D.; Kingsbury, D. B.; Garrison, B. J. *Appl. Surf. Sci.* **2006**, *252*, 6463.
- (19) Webb, R.; Kerford, M.; Way, A.; Wilson, I. *Nucl. Instrum. Methods Phys. Res., Sect. B* **1999**, *153*, 284.
- (20) Russo, M. F., Jr.; Wojciechowski, I. A.; Garrison, B. J. *Appl. Surf. Sci.* **2006**, *252*, 6423.
- (21) Russo, M. F., Jr.; Szakal, C.; Kozole, J.; Winograd, N.; Garrison, B. J. *Anal. Chem.* **2007**, *79*, 4493.

recombination energy was artificially high, and the resulting information could only be used as an indicator of where reactions might occur. In the benzene and polymer calculations the technique of coarse-graining was used to combine hydrogen atoms with their nearest bonded carbon atom to create CH_x particles. Coarse-graining decreases computation time by using simpler potentials, reducing the number of particles in a simulation, and eliminating the hydrogen vibration but also limits the number of chemical reactions that can be modeled.

In order to model of broad range of chemical reactions in a simulation, more complex potentials need to be employed which also increase computation time. It is prudent, then, to utilize models and concepts that allow us to focus on important time and space regions for elucidating the effects of chemistry on the dynamics. The mesoscale energy deposition footprint (MEDF) model^{21,26,27,30,31} predicts that the energy deposition profile at the time when most of the projectile energy has been deposited to the sample can be used to predict information about the trends in yields. From previous simulations,^{21,27,30,31} it is clear that the projectile energy is deposited in an approximately cylindrical track in the sample within the first few hundred femtoseconds of a trajectory creating a fluid-like motion of the sample particles. The particles that are within a depth that is equal to the width of the cylinder are ejected upward as well as some of the particles in the near-surface region that are outside the energized cylinder. This creates an ejection cone of material. Calculations on water ice,²² benzene,³² and polyethylene²⁸ show that the reaction region is within the conical volume.

The objective of this study is to address how energy is deposited into the sample when the sample molecules can undergo a broad range of chemical reactions, thus providing multiple avenues for energy deposition, and what effect this will have on the resulting ejection dynamics. The approach taken is to use MD simulations as it provides a microscopic view of the events. We employ samples of octane and octatetraene crystals, which have similar masses but different coordination and crystallographic orientation. The AIREBO potential³³ is selected since it allows for chemical reactions to occur in hydrocarbon molecules. Simulations of C_{60} bombardment are performed with projectile energies of 5, 10, and 20 keV.

The crystallographic structure of each system affects where the projectile energy is deposited and therefore how many molecules may react. The octatetraene system yields more reacted molecules following bombardment, whereas the octane molecules

are, on average, more dissociated. In both cases, several free and reacted H atoms are released into the plume and the crater walls. In addition, the simulations show how intact molecules of both systems may be ejected with low internal energies.

DESCRIPTION OF THE CALCULATION

There are several considerations when designing an appropriate calculation. In principle, it would be desirable to have molecules that represent typical analytes used in experiment and not small molecules like water. We do, however, want a sufficient number of molecules to eject, and it has been shown previously²⁸ that if the molecules are too large, then the ejection yields dramatically decline. The C_{60} bombardment process will create numerous bond cleavages;²² thus, the interaction potential or forces among the atoms and molecules must describe reasonable chemistry including dissipation of energy into this channel. Finally, the overall system size and time used in the simulation must be computationally tractable. These criteria are not mutually compatible; thus, the following strategy is employed.

A realistic description of internal modes including dissociation is required. One suitable available potential is the AIREBO potential³³ which includes long-ranged interactions in addition to the short-ranged chemical properties of the Brenner REBO potential.^{34,35} Thus, the chosen molecule is restricted to C and H atoms. Therefore, as moderate-sized molecules, octane (C_8H_{18}) and *trans,trans*-1,3,5,7-octatetraene (C_8H_{10}) are chosen. These two molecules both have eight C atoms and are linear molecules. They differ, however, in the number of H atoms. The C atoms in octane are fully saturated, whereas octatetraene has alternating double and single bonds. Octane crystallizes into a triclinic structure,³⁶ and octatetraene crystallizes into a monoclinic structure.³⁷

We assume that the dynamics of emission of the molecules follows the same basic process as found in other simulations. This assumption is necessary because the sample size needed for even 5 keV C_{60} bombardment of molecular benzene is 350 Å wide by 200 Å deep,²⁵ a size that is computationally intractable²⁴ using the atomistic AIREBO potential. The important concepts from prior simulations on organic solids are that most of the energy of the C_{60} is deposited within approximately 100–200 fs,^{21,25,30,31} there is a period of approximately 500–1000 fs in which chemical reactions transpire,²² and the material flows from the surface.^{21,30,31} Thus, we will only follow the initial phase of the molecular motion up to 1500 fs because the reactions should be completed and the motion of ejection initiated. An animation for several picoseconds of 5 keV C_{60} bombardment on a simplified representation of a benzene solid is given as animation 3 in previously published work.¹²

The molecular solids of octane and octatetraene were generated with the program CrystalMaker³⁸ using the experimental

- (22) Ryan, K. E.; Wojciechowski, I. A.; Garrison, B. J. *J. Phys. Chem. C* **2007**, *111*, 12822.
- (23) Ryan, K. E.; Smiley, E. J.; Winograd, N.; Garrison, B. J. *Appl. Surf. Sci.* **2008**, *255*, 844.
- (24) Smiley, E. J.; Postawa, Z.; Wojciechowski, I. A.; Winograd, N.; Garrison, B. J. *Appl. Surf. Sci.* **2006**, *252*, 6436.
- (25) Smiley, E. J.; Winograd, N.; Garrison, B. J. *Anal. Chem.* **2007**, *79*, 494.
- (26) Ryan, K. E.; Garrison, B. J. *Anal. Chem.* **2008**, *80*, 5302.
- (27) Ryan, K. E.; Garrison, B. J. *Anal. Chem.* **2008**, *80*, 6666.
- (28) Delcorte, A.; Garrison, B. J. *J. Phys. Chem. C* **2007**, *111*, 15312.
- (29) Delcorte, A.; Wehbe, N.; Bertrand, P.; Garrison, B. J. *Appl. Surf. Sci.* **2008**, *255*, 1229.
- (30) Russo, M. F., Jr.; Garrison, B. J. *Anal. Chem.* **2006**, *78*, 7206.
- (31) Russo, M. F., Jr.; Ryan, K. E.; Czerwinski, B.; Smiley, E. J.; Postawa, Z.; Garrison, B. J. *Appl. Surf. Sci.* **2008**, *255*, 897.
- (32) Czerwinski, B.; Rzeznik, L.; Paruch, R.; Garrison, B. J.; Postawa, Z. *Nucl. Instrum. Methods Phys. Res., Sect. B*, submitted for publication, **2008**.
- (33) Stuart, S. J.; Tutein, A. B.; Harrison, J. A. *J. Chem. Phys.* **2000**, *112*, 6472.

- (34) Brenner, D. W.; Shenderova, O. A.; Harrison, J. A.; Stuart, S. J.; Ni, B.; Sinnott, S. B. *J. Phys.: Condens. Matter* **2002**, *14*, 783.
- (35) Brenner, D. W. *Phys. Rev. B* **1990**, *42*, 9458.
- (36) Mathisen, H.; Norman, N.; Pedersen, B. F. *Acta Chem. Scand.* **1967**, *21*, 127.
- (37) Baughman, R. H.; Kohler, B. E.; Levy, I. J.; Spangler, C. *Synth. Met.* **1985**, *11*, 37.
- (38) CrystalMaker: A Crystal and Molecular Structures Program for Mac and Windows; CrystalMaker Software Ltd.: Oxford, England, 1994 (www.crystallmaker.com).

crystal structures. The systems were cropped to samples approximately 180 Å wide and 120 Å deep. For octane, there are 18 239 molecules or 474 214 atoms for a density of 0.9 g/cm³. For octatetraene, there are 21 376 molecules or 384 768 atoms for a density of 1 g/cm³. Due to the crystal structures and the arbitrary axis system used in the cropping process, the octane system has the molecular chains oriented approximately parallel to the surface, and the octatetraene system has the molecular chains oriented approximately 30–40° with respect to the surface normal. The effect of these orientations is obvious in the figures. With the use of the AIREBO potential, the cohesive energy of octane is 0.56 eV and that of octatetraene is 0.50 eV. These values are similar to those for ice and benzene, two systems we have modeled previously. A rigid region of 10 Å encases five sides of the sample with an inner stochastic layer of 20 Å. The C₆₀ bombards at normal incidence to the surface with an energy of 5, 10, or 20 keV.

In the analysis given below, estimation of internal energy of the desorbed molecules is important for interpreting experimental observations. Vibrational transitions, especially the higher energy bond stretch modes, are inherently quantum mechanical, however. Within a classical description of atomic motions, a small collision can increase the vibrational energy of a molecule without giving it a full quantum of energy. Quantum mechanically, this process is not allowed, which is why simulations of liquid solutions or biological molecules constrain bond lengths at the equilibrium distance. For us to use this fixed bond length constraint, however, means that molecules could not dissociate, an important energy dissipation mechanism for C₆₀ bombardment. Thus, our calculations overestimate the amount of internal energy going to the molecules and thus presumably underestimate the amount of center-of-mass kinetic energy of the intact molecules. The precise degree of overestimation of internal energy cannot be determined. For reference, the molecules octatetraene and octane have 48 and 72 vibrational modes, respectively. The energy required to excite every vibrational mode in octatetraene with one quantum of energy is ~8 eV and that of octane is approximately 60% larger as estimated by electronic structure calculations of each molecule.

RESULTS AND DISCUSSION

We start the discussion first with time snapshots of the motion, then discuss the energetics and reactions, followed by an analysis of the internal energy of ejected molecules. Time snapshots for the simulations of 20 keV C₆₀ bombardment of octane and octatetraene are shown in Figure 1. Only molecules whose center-of-mass is in a 20 Å wide slice directly below the C₆₀ impact point are shown except for one frame which is a top-down view of all of the atoms. For the coloring of the molecules, the center-of-mass kinetic energy is calculated for each molecule and subtracted from the total energy in order to obtain the change in internal energy. Atoms in molecules that react (dissociate, bond to another molecule or to C₆₀ atoms) are gray. These molecules (or fragments) are shown in all snapshots as they visually delineate the crater region. The red, orange, and yellow molecules have greater than 4 eV, between 2 and 4 eV, and between 0.05 and 2 eV of internal energy, respectively, have a center-of-mass velocity component upward, and have a center-of-mass kinetic energy greater than 0.5 eV, approximately the

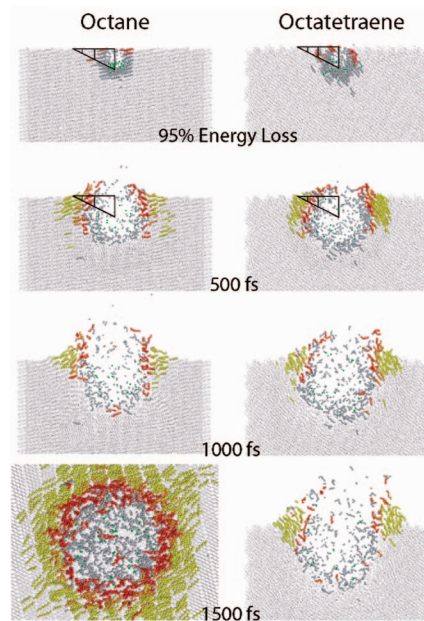


Figure 1. Snapshots of the atomic positions subsequent to C₆₀ bombardment at 20 keV on octane and octatetraene. Only the molecules whose center-of-mass (com) is within a 20 Å wide slice centered on the impact point of the C₆₀ molecule are shown. The 95% energy loss time for octane is ~60 fs, and that for octatetraene is ~70 fs. The 1500 fs snapshot for octane is a top-down view. Animations of both systems in a side view and in top-down or planview are included in the Supporting Information. The triangles represent the predicted ejection cones with a height of 20 Å and base radius of 40 Å. Lines are also drawn at 20 and 30 Å from the center of the sample. The color scheme is as follows: big spheres represent C atoms, and small spheres represent H atoms; green spheres are C atoms in original C₆₀; gray spheres are atoms in molecules that have reacted; red spheres are atoms within molecules with a change of greater than 4 eV of internal energy, moving up, and have com kinetic energy >0.5 eV; orange spheres are atoms within molecules with a change of 2–4 eV of internal energy, moving up, and have com kinetic energy >0.5 eV; yellow spheres are atoms within molecules with a change of 0.05–2 eV of internal energy, moving up, and have com kinetic energy >0.5 eV; all the rest of the atoms (moving down, not reacted, or <0.5 eV of kinetic energy) are little dots.

cohesive energy of the molecules in the solid. This last criterion selects for molecules that are candidates for ejection. All of the rest of the atoms are shown as small dots except for the C atoms from the C₆₀ molecule which are shown in green. Proceeding stepwise through the evolution of the simulation, the first frame shows the configuration when ~95% of the incident energy has been deposited into the system, 60 fs for octane and 70 fs for octatetraene. Snapshots are also shown at 500, 1000, and 1500 fs. In addition to still snapshots in Figure 1, there are side view and top-down or planview animations in the Supporting Information for both octane and octatetraene. For several of the discussion points below, the animations are essential for viewing the events.

The critical issue for understanding many of the results is the placement of the energy of the C₆₀ projectile into the substrate. In previous studies for simulations on atomic-like solids, we have developed a protocol for using quantitative information about the energy deposited to predict yields with the MEDF model.^{21,26,27,30,31} This model assumes that the deposited energy

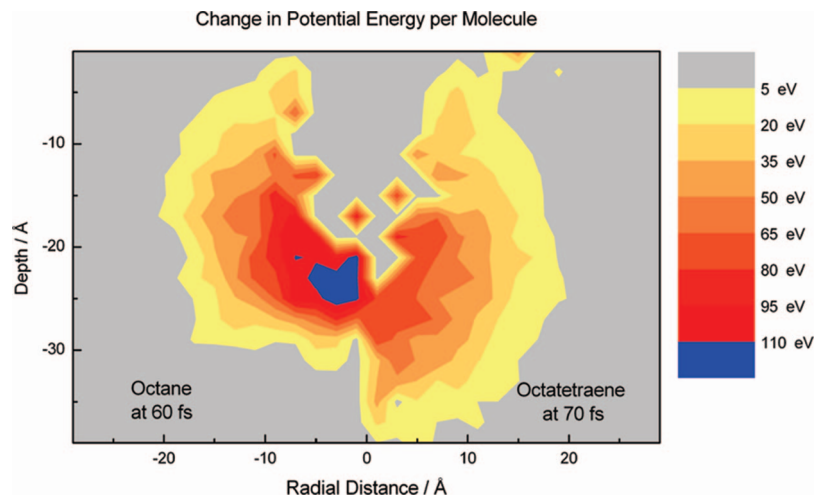


Figure 2. Contour plot of the change in potential energy per molecule for the octane (left) and octatetraene (right) systems at the time when 95% of the initial 20 keV of energy has been deposited in the substrate. The data are collected assuming cylindrical symmetry.

initiates a fluid flow from the substrate.³⁹ The partitioning of energy will be discussed below, but in this study, half of the incident energy increases the potential energy of the molecules, many of which dissociate or react with other species. It is not clear how this energy participates in the overall flow motion of the substrate toward the vacuum. Consequently, we use the principles of the MEDF model to examine the placement of energy in the system but refrain from quantitative analyses.

The placement of energy in the substrate is shown as potential energy contour plots in Figure 2 for the octane (left) and octatetraene (right) systems at the time when 95% of the projectile energy has been deposited in the substrate. The choice of which energy (e.g., potential, total) to use for the plot does not alter the determination of where the energy is deposited. The plot has been smoothed by collecting the data for each molecule and placing it at the positions of each C atom in the molecule.

The dynamics of bombardment is very similar for the two systems and is similar to previous simulations on molecular targets.^{20,25,30} Specifically, the dynamics reveals when and where the energy is deposited and the initiation of flow from the surface. This information is shown in Figure 1 and especially in the animations in the Supporting Information. As found for many similar systems,^{21,23,26,27,30,31} the energy is deposited in a region of radius about 20 Å. The crystallography and orientation of the molecules has an impact on the cluster bombardment process, however. For octane, where the molecular chains are oriented nearly parallel to the surface, the energy deposition is confined to a depth of 30 Å. The molecules in the octatetraene system are oriented approximately 30–40° with respect to the surface normal. Here, the energy is deposited to a depth of about 40 Å. The difference in energy deposition is related to the arrangement of the molecules. As observed in recent simulations of C₆₀ bombardment of a coarse-grained representation of a Langmuir–Blodgett film,^{40,41} bombardment perpendicular to the chains, as in octane, more effectively stops the projectile motion, whereas bombard-

ment close to parallel to the chains, as in octatetraene, allows the C atoms in the C₆₀ cluster to penetrate deeper. Regardless of the slight differences in the two systems, the incident energy of the C₆₀ is deposited at the critical depth for maximizing emission of molecules.^{21,30,31}

These simulations allow for an analysis of how the energy from the incident projectile gets partitioned into various channels using an interaction potential that has an atomistic representation and describes reasonable chemistry. The two most comparable prior simulations include 5 keV simulations of benzene²⁷ described with a coarse-grained representation where each CH group is described by one particle and simulations on water ice^{22,42} using a potential that dissociates into ions but has an artificially large recombination energy.⁴² There are several common observations. In all three sets of simulations, most of the energy of the C₆₀ projectile is transferred to the substrate within at most ~100–200 fs. The time scale for the partitioning of the deposited energy into potential and kinetic energy changes of the entire system occurs until 300–400 fs. Reactions will occur up to 500–1000 fs. A graph of the time evolution of reactions has been reported previously.²² The main difference between the current simulations and those for the coarse-grained benzene system is the amount of energy that may go into the potential energy of the molecules. For the coarse-grained benzene system,²⁷ there is only one type of bond, a CH–CH bond, that may be broken. The octane and octatetraene systems contain many C–H bonds and C–C bonds at different points on the chain which may all be broken and thus provide more avenues for projectile energy to be converted to potential energy. In addition, incident energy can be used not only to strain the molecules causing bond breaks, but also to compress the molecules, which occurs along the crater walls and will increase their potential energy. For these two C₈H_n systems, approximately 50% of the incident energy goes into changes in potential energy for all incident energies. As seen from Figure 2 initially the change in the potential energy of the molecules can be 10–100 eV. This large amount of energy means that any number of processes involving excited electronic states of the molecules or ionization events are energetically possible.²² The Brenner REBO potential^{34,35} only

(42) Wojciechowski, I. A.; Garrison, B. J. *J. Phys. Chem. B* **2005**, *109*, 2894.

(39) Jakas, M. M.; Bringa, E. M.; Johnson, R. E. *Phys. Rev. B* **2002**, *65*, 165425.

(40) Paruch, R.; Czerwinski, B.; Rzeznik, L.; Garrison, B. J.; Winograd, N.; Postawa, Z. *Nucl. Instrum. Methods Phys. Res., Sect. B*, submitted for publication, **2008**.

(41) Paruch, R.; Rzeznik, L.; Czerwinski, B.; Garrison, B. J.; Winograd, N.; Postawa, Z. *J. Phys. Chem. C*, submitted for publication, **2008**.

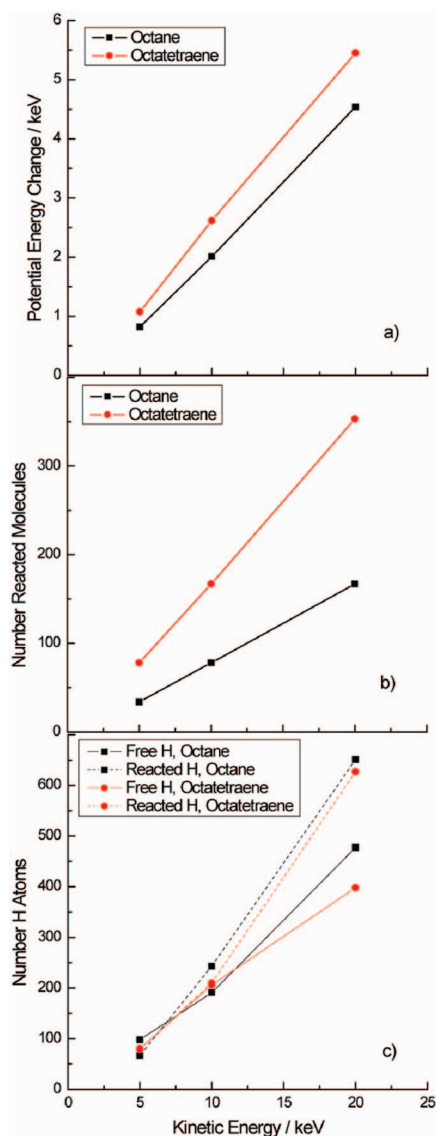


Figure 3. Reaction properties at 1500 fs as a function of incident kinetic energy for the octane and octatetraene systems. Red lines/symbols are for octane, and black lines/symbols are for octatetraene. (a) Change in potential energy of the molecules that react. (b) Number of molecules that react. (c) Number of free H atoms (solid lines) and number of H atoms reacted with another molecule or part of the C_{60} (dashed lines).

describes, at best, reactions on the ground electronic state; thus, it is not feasible to predict all the reaction products. We can, however, estimate the number of reacted molecules, their original position in the substrate, and the fate of reacted H atoms.

There are different measures for the number of reactions ensuing for each system. One measure is the amount of energy deposited in the reacted molecules as shown in Figure 3a using the potential energy. A second measure is the number of reacted molecules as shown in Figure 3b. Reacted molecules can be those that have dissociated or bonded to another molecule or C atoms from the projectile. The potential energy change is about the same for both systems, but the number of reacted octatetraene molecules is about twice the number of reacted octane molecules. The factor of 2 difference is attributable to the nature of the energy deposition shown in Figure 2 where the energy in the octatetraene system is more spread out, thus affecting more molecules. The

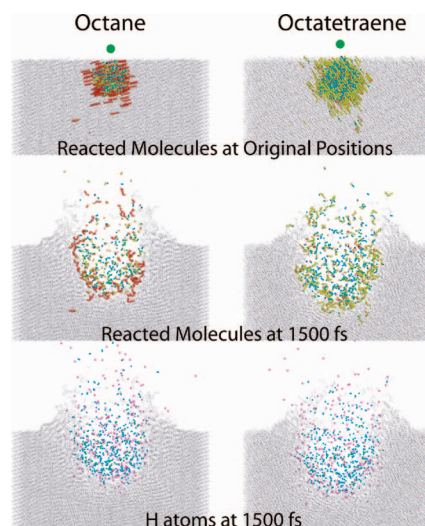


Figure 4. Snapshots showing reactions for 20 keV bombardment. Only the molecules whose center-of-mass is within a 40 Å wide slice centered on the impact point of the C_{60} molecule are shown. The top two panels show the C atoms in the molecules that react at their original positions and at 1500 fs. Green spheres are for the C_{60} atoms, red, yellow, cyan, orange, and blue spheres represent atoms with fourfold, threefold, twofold, onefold, and no coordination, respectively. The bottom panels show the free H atoms (magenta) and H atoms (cyan) bound to a different molecule at 1500 fs.

octane molecules are on average more dissociated than the octatetraene molecules, consistent with a similar amount of energy going into each system at a particular incident energy as shown in Figure 3a.

The initial positions of the majority of the reacted molecules, shown in the top frames of Figure 4, correlate with the volume where the energy was deposited as shown in Figure 2. The coloring of the carbon atoms is by coordination although at this time there is no obvious significance to the various coordination numbers. The energy is more spread out for octatetraene, and thus the volume where molecules react is larger. In both systems, there are a handful of molecules away from the crater that have reacted. The positions of the reacted molecules at 1500 fs, shown in Figure 4, are mostly in the plume and crater region. It is obvious that some of the reacted molecules are ejecting from the system. The fates of the molecules near the edges of the crater are uncertain given the limited time scale of the simulation and issues associated with limitations of the interaction potential for describing all possible reaction channels. They have not, however, penetrated deep into the sample.

The fate of H atoms is of potential importance to the SIMS community because the detected positively charged molecule is generally attached to a proton. It has been proposed^{43,44} that protons generated in one bombardment event provide part of the source of protons for the ionization event in subsequent impacts. We recognize that our H atoms are neutral, but it is illustrative to examine the number and fate of these atoms. Shown in Figure 3c are the number of free H atoms and number of H atoms bound to other molecules as a function of kinetic energy. The side view

(43) Conlan, X. A.; Lockyer, N. P.; Vickerman, J. C. *Rapid Commun. Mass Spectrom.* **2006**, *20*, 1327.

(44) Winograd, N.; Postawa, Z.; Cheng, J.; Szakal, C.; Kozole, J.; Garrison, B. J. *Appl. Surf. Sci.* **2006**, *252*, 6836.

animations in the Supporting Information show small gray dots (free H atoms) streaming off the surface from very early times. There is very little difference between the two C_8H_n systems. At 20 keV at 1500 fs, there are about 400 free H atoms and another ~ 700 H atoms bound to different molecules or atoms from the C_{60} . The positions of these H atoms at 1500 fs are shown in Figure 4, where magenta dots correspond to free H atoms and cyan dots to the reacted H atoms. Both groups of H atoms are in the ejecting material of the plume and in the crater region, and a few have penetrated into the substrate where there are no reacted molecules. There have been proposals that incident particles such as coronene⁴⁵ might enhance the number of available H atoms as potential ionization species. These simulations show that the impact event creates many more H atoms than could possibly be attached to the incident particle. Adding a few tens of H atoms to an incident particle would not appear to make a difference as the bombardment event is capable of dissociating hundreds of H atoms from the molecules. The essential issue for SIMS, however, is the creation of protons and the attachment of the protons to molecules that eject. The experimental molecular ion yield is estimated to be 10^{-2} or one ion per 100 C_{60} impacts.⁴⁶ The essential issue is determining when and where the ions are being created.

The ejected intact molecules are the critical component of the SIMS analysis. Since these simulations have only been calculated for 1500 fs, some inferences need to be made. The energy is deposited in a cylinder of radius approximately 20 Å (Figure 2), a dimension that corresponds to approximately the colored molecules of the first frames in Figure 1. The MEDF model predicts that the ejected molecules flow into the vacuum from a cone with a depth equivalent to the energy deposition radius, that is, ~ 20 Å. To determine the dimension of the top radius of the cone, one needs to know the amount of energy deposited that can lead to flow motion. The MEDF analysis for water ice²¹ and molecular benzene using a coarse-grained representation²⁷ suggest that the dimension of the base of the cone is 30–50 Å. Since we have more energy going into reactions, we limit our discussion to the region for molecular ejection of less than about 40 Å. The conical ejection region is outlined as a triangle in Figure 1 with lines denoting 20 and 30 Å from the center of the sample.

The critical region for ejection of intact molecules is the top region of the surface. Consequently we analyze the evolution of energy partitioning for concentric rings around the impact point of octane molecules that were originally in the top 20 Å of the sample as shown in Figure 5. Figure 5a gives the average internal energy per molecule for three rings: less than 20 Å, between 20 and 30 Å, and between 30 and 40 Å. These regions are marked in the top four frames of Figure 1. The average internal energy per molecule decreases dramatically as a function of distance from the impact point. The trend in the internal energy is reminiscent of the total energy transfer proposed by Benninghoven in the precursor model for atomic bombardment which says that the greatest amount of energy is transferred from the projectile to the sample directly below projectile impact. As the distance from the point of impact increases, the amount of energy transfer decays

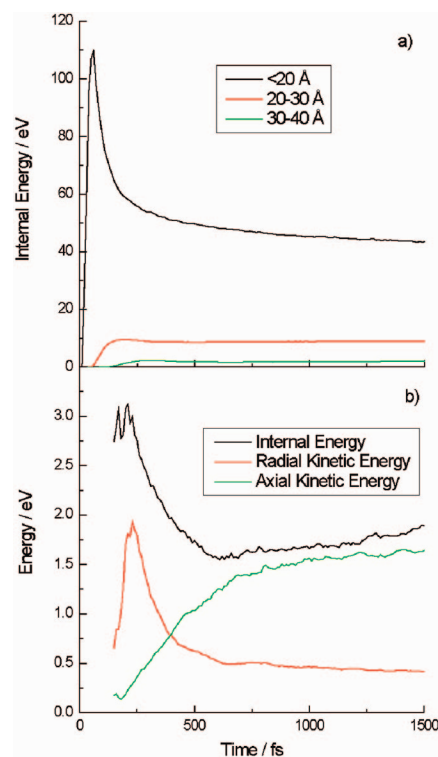


Figure 5. Energies for molecules originally in the top 20 Å for octane vs time for 20 keV bombardment. (a) Internal energy for molecules with center-of-mass within 20 Å of impact point (black), from 20–30 Å (red), and from 30–40 Å (green). (b) Internal energy (black), radial kinetic energy (red), and axial kinetic energy (green) for molecules with center-of-mass within 30–40 Å of impact and at the current time with center-of-mass energy >0.5 eV and moving up, the same criteria for yellow, orange, and red molecules in Figure 1.

to zero.⁴⁷ Interestingly, this model is more applicable to cluster bombardment than atomic bombardment in which there is a large diversity of action.⁴⁸ The molecules in the central region are obviously the ones that dissociate and react (the gray molecules in Figure 1 and the animations in the Supporting Information). The average internal energy of the molecules in the 20–30 Å ring is ~ 9 eV (the red molecules in Figure 1 and the animations in the Supporting Information). As given above, this amount of energy corresponds to less than one quantum of energy going into every vibrational mode of octane. Although it is sufficient to dissociate the molecule, it is improbable that all the energy will localize in a single bond. Finally, for the molecules in the 30–40 Å ring, the average internal energy is less than 2 eV, approximately the yellow molecules in Figure 1 and the animations in the Supporting Information. As discussed above, the classical approximation overestimates the amount of internal energy for these molecules. The second point that is obvious from Figure 5a is that for the molecules between 20–40 Å attain their internal energy within 200–300 fs which then remains nearly constant.

A more detailed analysis of the energy is given for the molecules in the 30–40 Å ring, that is, the most probable low internal energy ejected molecules, in Figure 5b. In this case, only the molecules that have more than 0.5 eV of center-of-mass kinetic energy and are moving up are counted in the averages at each

(45) Biddulph, G. X.; Piwowar, A. M.; Fletcher, J. S.; Lockyer, N. P.; Vickerman, J. C. *Anal. Chem.* **2007**, *79*, 7259.

(46) Cheng, J.; Winograd, N. *Anal. Chem.* **2005**, *77*, 3651.

(47) Benninghoven, A. *Int. J. Mass Spectrom. Ion Processes* **1983**, *53*, 85.

(48) Delcorte, A.; Garrison, B. J. *J. Phys. Chem. B* **2000**, *104*, 6785.

time. Thus, at the shortest times there are only a handful of molecules being considered, while at the longest times there are about 180 molecules. Given in the plot is the average internal energy per molecule, the average radial center-of-mass kinetic energy, and the average axial (upward) center-of-mass kinetic energy. The internal energy and the radial kinetic energy increase in a concerted manner, reaching a maximum at ~ 250 fs. At this time, since the molecules cannot compress further in the horizontal direction, they start moving toward the vacuum, and the axial kinetic energy increases. The timing of the energy partitioning is completely consistent with our picture developed from simulations of more atomic-like systems of an energized track followed by material flowing from the surface due to the vacuum above the surface.^{21,30,39} Initially the C_{60} energy goes toward moving the molecules horizontally, and then the molecules start moving toward the vacuum, that is, flowing off the surface. The perpendicular kinetic energy becomes larger than the horizontal kinetic energy. The snapshots in Figure 1 and the animations in the Supporting Information show graphically that the molecules attain their internal energy early in the process and keep approximately the same internal energy as they flow from the surface. Although the above analysis is based on average energies per molecule, the information for individual molecules follows the same trends.

Before discussing the experimental implications of the flow of molecules from the surface, it is useful to compare the response of these systems to that observed by atomic bombardment. First, it is not practical to run full simulations of atomic bombardment on these systems because a much larger sample would be needed and multiple impacts would have to be performed to obtain statistical reliability. For C_{60} bombardment, the motion is relatively uniform from one impact to the next.¹⁷ We did, however, model the initial stages of one impact each of Au and Ga bombardment of octatetraene at 10 keV using the sample sizes discussed above. Previous simulations of C_{60} and Au_3 on water ice^{21,30} and benzene using a coarse-grained representation²⁶ consistently show that the critical depth for depositing energy is 20–30 Å to be useful for promoting ejection. When the Au and Ga projectiles have penetrated 30 Å into the octatetraene, they have deposited 17% and 31%, respectively, of their initial energy, whereas the C_{60} has deposited all of its energy. The amount of energy deposited by the atomic projectiles in the critical region is considerably less than the C_{60} projectile, consequently the yields will be smaller.

These simulations demonstrate that C_{60} bombardment of molecular solids give rise to numerous molecules that can potentially eject (yellow, orange, and red molecules in Figure 1 and the animations in the Supporting Information) that have sufficiently low internal energy that they will not dissociate during the flight to the detector. Although the simulations have not been run long enough to determine an actual number of ejected molecules, any of the colored molecules have, in principle, a sufficient amount of center-of-mass kinetic energy that they can overcome any binding interactions to other molecules. The simulations clearly show that the molecules attain their internal energy within the first 200–300 fs after the impact and then flow off the surface maintaining their internal energy. This mechanism is in contrast to a collisional cooling mechanism that has been

proposed for cluster bombardment^{10,11,49} in which the molecules undergo collisions in the plume and thus lose internal energy. In fact, the central area of the plume (Figure 1) contains mainly the fragmented and reacted species. The molecules with lower internal energies are at the edges of the motion and will not participate in collisional cooling.

The prediction that C_{60} bombardment of a molecular solid will eject numerous molecules that already possess low internal energies rather than undergoing collision cooling in the plume explains recent experimental results by Willingham et al.⁵⁰ in which they used laser irradiation to ionize ejected neutral molecules. Previous attempts to use laser postionization approaches for ionizing molecules ejected in atomic SIMS had been met with frustration because the ejected molecules had too much internal energy and readily dissociated.^{50,51} The Willingham experiments, however, found that not only does C_{60} bombardment create a higher ejection yield but also a higher yield of intact molecular species.⁵⁰ These calculations clearly show how molecules can eject with low internal energies, making them less likely to dissociate upon laser irradiation.

The other relevant experiment involves the combined technologies^{52–54} of C_{60} bombardment with a QSTAR XL instrument (Applied Biosystems/MDS Sciex) designed for laser ablation or matrix-assisted laser desorption ionization (MALDI) studies.^{9,52,55} In this experimental configuration, secondary ions pass through a region of N_2 gas in order to cool the ejected molecules. These new experiments demonstrate that the intact molecular ion yield is larger with the presence of the cooling gas.⁵⁶ These calculations clearly show that there are a range of internal energies of the ejected molecules as noted by the yellow, orange, and red colors in Figure 1 and the animations in the Supporting Information; thus, there are molecules whose internal energy can be reduced.

A correlation between the internal energies of the molecules versus initial horizontal distance from the C_{60} impact is implied from Figure 1, the animations in the Supporting Information, and Figure 5. This correlation suggests that one might design experiments with either thermometer molecules or molecules with many isomerization channels for the substrate. Comparison between targets consisting of isomer molecules with the same molecular mass but different ionization or thermal characteristics could demonstrate that cooler molecules come from the edges of the impact region. It would be expected that the yields of these materials should be similar, but there should be a geometrically predictable change in the ratio of fragmented to intact molecular emission based on the energy spread of the ejection cone.

(49) Garrison, B. J. *Appl. Surf. Sci.* **2006**, 252, 6409.

(50) Willingham, D.; Kucher, A.; Winograd, N. *Appl. Surf. Sci.* **2008**, 255, 831.

(51) Vorsa, V.; Willey, K. F.; Winograd, N. *Anal. Chem.* **1999**, 71, 574.

(52) Carado, A.; Kozole, J.; Passarelli, M.; Winograd, N.; Loboda, A.; Wingate, J. *Appl. Surf. Sci.* **2008**, 255, 1610.

(53) Carado, A.; Passarelli, M. K.; Kozole, J.; Wingate, J. E.; Winograd, N.; Loboda, A. V. *Anal. Chem.* **2008**, 80, 7921.

(54) Carado, A.; Kozole, J.; Passarelli, M.; Winograd, N.; Loboda, A.; Bunch, J.; Wingate, J.; Hankin, J.; Murphy, R. *Appl. Surf. Sci.* **2008**, 255, 1572.

(55) Loboda, A. V.; Krutchinsky, A. N.; Bromirski, M.; Ens, W.; Standing, K. G. *Rapid Commun. Mass Spectrom.* **2000**, 14, 1047.

(56) Carado, A.; Winograd, N. Unpublished data, 2009.

CONCLUSION

Molecular dynamics simulations of the initial states of 5–20 keV C_{60} bombardment of molecular solids of octane and octatetraene have been performed employing an atomistic interaction potential that describes chemical reactions. These simulations allow for a description of how the incident energy is partitioned among the various modes and the nature and position of the reactions that can occur. Similarities between both systems exist in terms of where the incident energy is deposited in the sample, the amount of energy going into the reactions, the small number of reacted molecules below the crater, and the number of H atoms available for reactions. The incident energy is deposited in the near-surface region in a cylinder of radius approximately 20 Å and to a depth of 30–40 Å. Approximately half of the incident energy goes into changes in potential energy of the molecules with half of this amount going to molecules that react, that is, either dissociate or react with other molecules or atoms from the C_{60} cluster. The molecules that react originate for the most part in the cylinder region where the energy is deposited. At 1500 fs, the reacted molecules are in the ejected plume, in the crater region, and near the edges of the crater. At 20 keV, there are ~350 octatetraene molecules that have reacted and ~150 octane molecules that have reacted. The differences in the numbers reflect the crystallography of the two systems with respect to the effectiveness in stopping the incident C_{60} projectile with the octane molecules being, on average, more fragmented than the octatetraene molecules. Also at 1500 fs, there are about 400 free H atoms and over 600 H atoms that have reacted with other molecules. Both types of H atoms are spread through the plume, crater, and edge of the crater regions.

The dynamics of the energy flow show clearly that in the top surface region, from where intact molecules will eject, initially the energy goes to increases in potential and radial kinetic energy before 200–300 fs. Then the axial kinetic energy increases causing the molecules to flow from the surface. This description of ejection of material is consistent with that found for atomic systems and

demonstrates that we can use previously developed concepts of emission due to cluster bombardment for organic solids. The calculations show a correlation between the amount of internal energy of molecules that are about to eject with distance from the C_{60} impact point, demonstrating that there are tens to hundreds of molecules that can eject with low internal energies. This observation is consistent with recent experiments of laser postionization of emitted molecules.

ACKNOWLEDGMENT

The authors thank Arnaud Delcorte for helpful scientific discussions as well as Pat Conforti and Mike Russo for their help with graphics. For financial support, Z.P. acknowledges the Polish Ministry of Science and Higher Education program nos. PB 4097/H03/2007/33 and N N204 093535; B.J.G. and K.E.R.—the National Science Foundation Grant CHE-0456514; N.W.—the National Institutes of Health Grants EB002016-13 and GM069338, the National Science Foundation Grant CHE-0555314, and the Department of Energy Grant DE-FG02-06ER15803; and R.P.W.—the U.K. Engineering and Physical Sciences Research Council (EPSRC) Grant EP/C008251/1. We also recognize the support provided by the U.K. EPSRC under its Collaborating for Success through People initiative Grant EP/FO12985/1 for supporting prolonged exchange visits between Manchester, Surrey, and Penn State during which some of the ideas underlying this work were developed. Computational support was provided by the Graduate Education and Research Services (GEARS) group of Academic Services and Emerging Technologies (ASET) at Pennsylvania State University.

SUPPORTING INFORMATION AVAILABLE

Additional information as noted in text. This material is available free of charge via the Internet at <http://pubs.acs.org>.

Received for review November 12, 2008. Accepted January 23, 2009.

AC802399M